Fluorescence lifetime imaging microscopy (FLIM) to demonstrate the nuclear binding of flavanols and (--epigallocatechin gallate

Article

Accepted Version

Two-photon excitation with pico-second fluorescence lifetime imaging to detect nuclear association of flavanols

Irene Mueller-Harvey [a,*], Walter Feucht [b], Juergen Polster [c], Lucie Trnková [d], Pierre Burgos [e], Anthony W. Parker [e], Stanley W. Botchway [e]

[a] *Chemistry & Biochemistry Laboratory, Food Production & Quality Research Division, School of Agriculture, Policy & Development, University of Reading, P O Box 236, Reading RG6 6AT, UK*
[b] *Department of Plant Sciences, Technical University of Munich (TUM) Wissenschaftszentrum Weihenstephan (WZW), D-85354 Freising, Germany*
[3] *Department of Physical Biochemistry, Technical University of Munich (TUM), Wissenschaftszentrum Weihenstephan (WZW), D-85354 Freising, G*ermany
[4] *University of Hradec Králové, Faculty of Science, Department of Chemistry, Rokitanského 62, 50003 Hradec Králové, Czech Republic*
[5] *Central Laser Facility, Research Complex at Harwell, Science and Technology Facilities Council, Rutherford Appleton Laboratory, Harwell - Oxford, Didcot, OX11 0QX, UK*

Corresponding author. Tel.: +44 (0)118 378 6619; fax: +44 (0)118 935 2421.
E-mail address: i.mueller-harvey@reading.ac.uk;

E-mail addresses of co-authors:
Walter Feucht: walter.feucht@gmail.com
Juergen Polster: j.polster@wzw.tum.de
Lucie Trnková: lucie.trnkova@uhk.cz
Pierre Burgos: pierre.burgos@stfc.ac.uk
Anthony W. Parker: tony.parker@stfc.ac.uk
Stanley W. Botchway: stan.botchway@stfc.ac.uk

Keywords: Fluorescence lifetime imaging microscopy, flavanols, epigallocatechin gallate, nuclear binding, histone proteins, multiphoton excitation.

Two-photon excitation with pico-second fluorescence lifetime imaging to detect nuclear association of flavanols

Irene Mueller-Harvey [a,*], Walter Feucht [b], Juergen Polster [c], Lucie Trnková [d], Pierre Burgos [e], Anthony W. Parker [e], Stanley W. Botchway [e]

[a] *Chemistry & Biochemistry Laboratory, Food Production & Quality Research Division, School of Agriculture, Policy & Development, University of Reading, P O Box 236, Reading RG6 6AT, UK*

[b] *Department of Plant Sciences, Technical University of Munich (TUM), Wissenschaftszentrum Weihenstephan (WZW), D-85354 Freising, Germany*

[c] *Department of Physical Biochemistry, Technical University of Munich (TUM), Wissenschaftszentrum Weihenstephan (WZW), D-85354 Freising, Germany*

[d] *University of Hradec Králové, Faculty of Science, Department of Chemistry, Rokitanského 62, 50003 Hradec Králové, Czech Republic*

[e] *Central Laser Facility, Research Complex at Harwell, Science and Technology Facilities Council, Rutherford Appleton Laboratory, Harwell - Oxford, Didcot, Oxfordshire, OX11 0QX, UK*

ABSTRACT

Two-photon excitation enabled for the first time the observation and measurement of excited state fluorescence lifetimes from three flavanols in solution, which were ~ 1.0 ns for catechin and epicatechin, but <45 ps for epigallocatechin gallate (EGCG). The shorter

lifetime for EGCG is in line with a lower fluorescence quantum yield of 0.003 compared to catechin (0.015) and epicatechin (0.018).

In vivo experiments with onion cells demonstrated that tryptophan and quercetin, which tend to be major contributors of background fluorescence in plant cells, have sufficiently low cross sections for two-photon excitation at 630 nm and therefore do not interfere with detection of externally added or endogenous flavanols in *Allium cepa* or *Taxus baccata* cells. Applying two-photon excitation to flavanols enabled 3-D fluorescence lifetime imaging microscopy and showed that added EGCG penetrated the whole nucleus of onion cells. Interestingly, EGCG and catechin showed different lifetime behaviour when bound to the nucleus: EGCG lifetime increased from <45 to 200 ps, whilst catechin lifetime decreased from 1.0 ns to 500 ps. Semi-quantitative measurements revealed that the relative ratios of EGCG concentrations in nucleoli associated vesicles : nucleus : cytoplasm were *ca.* 100:10:1.

Solution experiments with catechin, epicatechin and histone proteins provided preliminary evidence, via the appearance of a second lifetime (τ_2 = 1.9 to 3.1 ns), that both flavanols may be interacting with histone proteins. We conclude that there is significant nuclear absorption of flavanols. This advanced imaging using two-photon excitation and biophysical techniques described here will prove valuable for probing the intracellular trafficking and functions of flavanols, such as EGCG, which is the major flavanol of green tea.

Keywords: Fluorescence lifetime imaging microscopy, flavanols, epigallocatechin gallate, nuclear association, histone proteins, multiphoton.

1. Introduction

Plants synthesise >4000 different flavonoid compounds, which can be grouped into several different subgroups. Flavanols (Fig. 1) are an important subgroup that is widespread in plants and plant foods [1]; they are also precursors of condensed tannins, which are the fourth largest group of natural plant products after cellulose, hemicellulose, and lignin [2]. These polyphenolic compounds are attracting considerable interest, because diets rich in fruits and vegetables are associated with improved health and a reduction of age-related diseases such as cancer, osteoporosis and cardiovascular diseases [3-7]. Flavonoids are considered to be 'lifespan essentials' and recent reviews suggest that their antioxidant properties alone are unlikely to explain their beneficial effects on human health or their functions in plants [8-10].

A consensus is emerging that *in vitro* and *in vivo* experiments need to probe the bioavailability of these polyphenols and their molecular targets [3,6,8,10-11]. *In vitro* studies have tended to require 10 to 100-fold higher polyphenol concentrations than are usually found in mammalian plasma and tissues in order to achieve many of the reported medicinal effects [5,12]. However, the existence of high-affinity targets for dietary polyphenols might explain their health-promoting effects and in this context it is pertinent to examine more closely recent evidence that nuclei from both plant *and* mammalian cells acted as sinks for flavanols [13-17]. Although the function of these secondary plant

metabolites requires further elucidation, evidence is emerging that they may be important in cell development. For example, loss of flavanols has been linked to defective pollen development [14]. Different types of flavanol distribution patterns were observed in *Tsuga canadensis* at the sub-nuclear level [13] and the authors questioned whether the epigenetic code of histones could affect flavanol-chromatin associations. Moreover, Feucht *et al*. [15] found identical flavanol patterns within different cell lineages in a meristematic plant tissue and suggested that this could be indicative of a synchronized, transcriptional regulation. In addition, nuclear flavanol concentrations clearly depended on the season, i.e. during dormancy they were almost absent but during growth periods relatively high amounts were observed [18]. The fact that flavanols were associated with both interphase and mitotic chromosome states posed the question of whether flavanols might be associated with histones. If this is the case, then this could open a new perspective on genomic regulation.

This research by Feucht's group made use of the fact that flavanols form a blue condensation product with dimethylaminocinnamaldehyde (DMACA) [19]. The DMACA reagent is, however, a relatively aggressive reagent that requires 0.75 M sulfuric acid for the staining reaction and this could cause some physical damage within the cells. Polster *et al.* [18], therefore, tested the existence of nucleus-bound flavanols with a milder technique, i.e. laser microdissection and pressure catapulting (LMPC), which separated intact nuclei from cells and these also stained blue in the subsequent DMACA reaction. Nevertheless, LMPC causes physical rupture of the cytoplasm that surrounds the nuclei and could have given rise to an artificial DMACA reaction. Moreover, histological studies with DMACA cannot distinguish between different flavanols or between flavanol monomers, oligomers or

polymers [19]. Techniques are therefore required that can establish the sub-cellular localisation, and concentrations therein, of flavanols to probe their functionality and metabolism in plant and mammalian cells.

Nifli *et al.* [29] recently applied confocal fluorescence microscopy to map the intracellular distribution of a major plant flavonol, i.e. quercetin (Fig. 1), which has a UV absorption λ_{max} of 372 nm. Quercetin revealed a specific fluorescence (488 nm_{ex}/500-540 nm_{em}) in the cellular environment at physiologically relevant concentrations (<5 μM), which the authors attributed to non-covalent binding to cellular components. Intracellular tracing of flavanols (λ_{max} ~ 280 nm; Fig. 1 and Fig. S1) by UV-Vis spectroscopy or confocal fluorescence microscopy is, however, not possible because plant and mammalian cells contain numerous compounds which would interfere with the detection of flavanols by giving background fluorescence signals (termed "auto-fluorescence"). Fig. 2 illustrates the photophysical processes in a conventional Jablonski diagramme, which depicts one- and two-photon excitation and various relaxation pathways that are open to the electronic excited state following photon(s) absorption.

In fluorescence life-time imaging microscopy (FLIM) both fluorescence intensities and fluorescence lifetimes of specific compounds can be measured at each pixel in the image [21,22]. In addition, variations in fluorescence lifetime can provide further image contrast: lifetime shifts can serve as sensitive probes for detecting molecular interactions and may yield information on a compound's environment, such as pH or oxygen concentration [23-25]. Lifetime, τ, is derived from the time-constant of the fluorescence decay (Fig. 2), where

$\tau = 1/k_{fluorescence}$. FLIM is based on either single- or multi-photon excitation techniques. Multi-photon excitation with femtosecond lasers offers many advantages for biological measurements over more conventional single photon excitation [23,26]:

- ✓Excitation with red light that is not directly absorbed by cellular materials.
- ✓Reduced cellular toxicity in biological studies.
- ✓Reduced photo-bleaching.
- ✓Deeper penetration of the near-infrared light into the biological specimen.
- ✓Femtolitre volume excitation.
- ✓A flexible imaging platform that is capable of resolving several (and related) compounds.
- ✓The ability to deliver UV-equivalent photon energies directly beneath UV absorbing materials and molecules.
- ✓An ability to perform time-resolved studies due to the short pulsed light source.

In two-photon excitation (2PE) the simultaneous absorption of two lower energy photons mimics the absorption of a single photon of equivalent higher energy (Fig. 2). Thus, 2PE at 560 nm mimics UV excitation at 280 nm [23,27]. In FLIM ultrafast lasers providing pulse lengths of the order of 200 femtoseconds (200×10^{-15} s) enable time-resolved measurements, which can detect molecular interactions in solution and cells [23-25,28] and can be used to construct fluorescence life-time maps of a compound's distribution within viable cells.

Here we describe 2PE experiments designed to eliminate any doubts regarding the results from previous histological studies that employed the DMACA staining reagent. Two-photon excitation coupled to 3-D fluorescence lifetime imaging microscopy enabled examination of intact biological tissues and highly localised, non-destructive and selective detection of flavanols. The fluorescence behaviour of three flavanols, catechin, epicatechin and epigallocatechin gallate (EGCG) (Fig. 1), was measured first in model solution systems and then in two natural cell systems, onion epidermis cells and *Taxus* pollen mother cells. These flavanols were chosen because they are widespread in plants and are also bioavailable and bioactive in several *in vitro* and *in vivo* mammalian cell systems [1,6,9,29]. Solution phase studies were first used to optimise and measure spectroscopic shifts and lifetime changes of free flavanols *versus* flavanols bound to DNA or histone proteins at normal physiological pH values. The optimised spectroscopic parameters were then applied to probe the intra-cellular location of externally added flavanols in *Allium cepa* cells and of endogenous flavanols in *Taxus baccata* cells. The same plant models had been tested previously with the DMACA staining reagent [14,30].

2. Methods and materials

2.1. Reagents

The following reagents were purchased from Sigma-Aldrich Company Ltd, UK: (+)-catechin (98%), (-)-epicatechin (90%), (-)-epigallocatechin gallate (95%; EGCG), tris-(hydroxymethyl)amino methane (Tris), K_2HPO_4 (ACS reagent, (≥ 98%), KH_2PO_4 (ACS reagent, (≥ 99%), DNA from calf thymus and Histone type II-A. Histone was supplied by Roche Diagnostics Ltd, UK. Histone sulphate from calf thymus was purchased from Fluka

(Sigma-Aldrich Chemie, Steinheim, Germany; Polster *et al.*, 2003). Ethanol (LiChrosolv, ≥ 99.9%) was purchased from VWR-Merck, UK.

Tris buffers (0.1 M) were prepared and adjusted to pH 7.0 and 8.0 with HCl and phosphate buffers (0.1 M) at pH 5.8, 7.1 and 8.2 were prepared using K_2HPO_4 and KH_2PO_4 as described [16].

2.2. Calculation of relative fluorescence quantum yields of the flavanols

Flavanols were dissolved in methanol to yield 0.01 M stock solutions. Subsequent dilutions for 20 and 40 μM flavanol concentrations were made with sodium phosphate buffer (pH 7.4, 0.1 M, 0.05% sodium azide). These were placed in a 10 mm quartz Suprasil fluorescence cuvette (Hellma, Germany) and UV-Vis spectra were first recorded from 190 to 500 nm using a Helios β spectrophotometer (Spectronic Unicam, U.K.). Then fluorescence spectra were recorded using a luminescence LS-55 spectrometer (Perkin Elmer, U.K.) from 290 to 530 nm with excitation at 295 nm under continuous stirring. The excitation and emission slits were both set to 5 nm and scanning speed was 200 nm min^{-1}. All experiments were carried out at 37 ^{o}C. The literature reported a quantum yield of 0.12 for tryptophan (Trp) at 270 nm (website) and we confirmed this for 295 nm. Therefore, the quantum yields of flavanols (Flav) were calculated relative to tryptophan using the integrated area between 300 and 530 nm under the fluorescence spectra [31-33] according to:

$$\text{Quantum yield}_{(\text{Flav})} = \frac{\text{Absorption at 295 nm (Trp)} * 0.12 * \text{Fluorescence (Flav)}}{\text{---}}$$

Absorption at 295 nm (Flav) * 0.12 * Fluorescence (Trp)

2.3. Flavanol solutions

Flavanols were dissolved in ethanol (~10 mM) and prepared fresh on a daily basis. Just before measuring the fluorescence lifetimes, aliquots (10 μL) were removed and diluted with buffer, DNA or histone protein solutions (90 and 40 μL) to obtain flavanol concentrations between 1 and 2 mM.

DNA (0.6 mg) was dissolved in Tris buffer (pH 8.0; 30 mL) overnight at 4 ^{o}C. Sigma histone (5.9 mg) was dissolved in Tris buffer (pH 7.0 and 8.0; 2.85 mL). Ethanol (98 μL) was added to the pH 8.0 buffer to facilitate dissolution. Histone sulphate (0.8 mg) was dissolved in Tris buffer (pH 7.0 and 8.0) according to Polster *et al.* [16]. The supernatants were used after centrifugation. Roche histone (1.0 mg) was dissolved in Tris buffer (pH 7.0 and 8.0; 500 μL) and ethanol (10 μL).

2.4. Plant samples

The thin adaxial epidermis from onion (*Allium cepa*) bulb scale was removed, cut into 2 cm^2 pieces and incubated with aqueous catechin or EGCG solutions (1 mM; 20 mL) for up to 8 h [30].

Male cones from yew (*Taxus baccata*) were harvested on 5th October 2008. The eight cover leaves were removed and the yellow anthers were gently squeezed with tweezers in order to release the mother pollen cells. Preliminary experiments revealed that these cells stained

dark blue with the DMACA reagent (10 mg DMACA dissolved in 1 mL of 0.75 M H_2SO_4) [30].

2.5. Multiphoton microscopy

The set up used in this study has been previously described [23]. Briefly, a custom built two-photon microscope was constructed using scanning XY galvanometers (GSI Lumonics Ltd). A diode-pumped (Verdi V18) titanium sapphire (Mira F900) operating at 700-980 nm generated laser light at a wavelength of 585 ± 2 nm and was used for the solution studies and at 630 ± 2 nm for the plant cell studies through an optical parametric oscillator (OPO, APE-Coherent GmbH, Berlin, Germany) operating at 180 fs pulses at 75 MHz. The pulse width was maintained using a femto control unit (APE Coherent GmbH). The laser beam was focused to a diffraction-limited spot using a water-immersion ultraviolet corrected objective (Nikon VC x60, NA 1.2) and specimens were illuminated at the microscope stage of a modified Nikon TE2000-U with UV transmitting optics. Fluorescence emission was collected without descanning, bypassing the scanning system, and passed through a 340 ± 20 nm interference filter (U340, Comar Instruments, Cambridge, UK). Emission fluorescence was detected using an external fast microchannel plate photomultiplier tube (Hamamatus R3809U-50) and recorded using a Time-Correlated Single Photon Counting (TCSPC) PC module SPC830 (Becker and Hickl GmbH, Berlin, Germany). Fluorescence lifetime image microscopy was performed by synchronising the XY galvanometer positions with the fluorescence decay. The X,Y galvanometers were raster scanned at 1 ms or 2 ms per pixel for 128 x 128 or 256 x 256 image size, respectively, giving a 33 sec per image

frame. The presented images were three accumulations to allow for enough photon counts per channel for the data analysis.

2.6. Image analysis

Steady state grey scale images (8 bit, up to 256 x 256 pixels) are produced by binning all decay photons as a single channel. Fluorescence lifetime images were obtained for control cells and flavanol-loaded cells by analysing the decay at individual pixels using a single or double exponential curve fitting (SPCImage 2.94 analysis software Becker and Hickl). A thresholding function within the FLIM analysis software ensured that noncorrelating photons leading to background noise arriving at the detector were not included in the analysis. Single point decay analysis was carried out without binning while FLIM was analysed with a maximum of 2 binning.

3. Results and discussion

3.1. Flavanol fluorescence lifetimes in aqueous solutions

It is well known that flavanols oxidise readily in alkaline pH [4], therefore lifetimes were first examined at pH values ranging from 5.8 - 8.2. Fig. 3 shows that the fluorescence lifetime, τ, of catechin (2 mM catechin solution in 0.1 M phosphate buffer) was relatively stable between pH 5.8 and 7.1: τ was 1.0 ns at the start and 0.9 ns after 20 min. However, at pH 8.2 the lifetime changed from 1.0 to 0.7 ns within 20 minutes. When the same measurements were conducted under a nitrogen blanket, lifetime reduction was kept to 9% over a 30 min period and this agrees with Sang *et al.* [34] who found that flavanols were not oxidised under nitrogen. Therefore, all subsequent solution measurements were

249 determined immediately after mixing the solutions, i.e. within 30 seconds. Fig. 3 also
250 shows that pH *per se* had no effect on catechin lifetimes: τ of catechin was ~1.0 ns at pH
251 5.8, 7.1 and 8.2. The reduction in τ values can also not be ascribed to sample concentration
252 or the presence of non-interacting or energy transfer products, as the excited state lifetime
253 is independent of both of these.
254
255 The natural lifetime of catechin in solution in the absence of oxygen is ~1.1 ns (Fig. 3).
256 This reduces, via quenching, as expected in the presence of dissolved oxygen (7.6 $mg \cdot L^{-1}$)
257 at room temperature and pressure to ~1 ns. It is worth noting that at high oxygen
258 concentrations, 30 mM, the quenched lifetime observed will be as expected taking into
259 account diffusion control rate. Therefore the subsequent change in lifetime (Fig. 3) (to ~0.7
260 ns after 20 min in oxygen) is very likely due to the formation of a deprotonated or oxidised
261 product as the OH groups in the B-ring are particularly susceptible to deprotonation and
262 therefore oxidation at alkaline pH [35]. It is interesting to note that the reduced lifetime
263 fitted well to a single exponential decay, again indicating a single fluorescent molecular
264 species is present and favouring the observed decreases in lifetime results from either a
265 photoproduct, which also fluoresces, or an oxygen quenched process. Further studies using
266 high performance liquid chromatography may help identify these oxidised products.
267
268 Importantly, Fig. 4 shows that flavanols had different fluorescent decay curves.
269 Fluorescence lifetimes of catechin and epicatechin were similar (1.0 and 1.1 ns,
270 respectively). However, in the case of EGCG at pH 8.1 (2 mM flavanol solutions in 0.1 M

phosphate buffer) the lifetime was found to be within the instrument response function and Fig. 4 shows only the characteristics of the fast micro-channel plate (<45 ps). Utrafast time-resolved Kerr gated fluorescence spectroscopy will be needed to resolve the EGCG lifetime in the future. EGCG differs from catechin and epicatechin by the presence of a galloyl group at C-3 (Fig. 1). The lifetime of the excited state is given by the sum of the different competing relaxation processes, which include fluorescence, non-radiative decay, intersystem crossing and chemical reaction as illustrated in Fig. 2. The shorter lifetime for EGCG is most likely due to the presence of additional phenolic groups, which would be expected to enhance the solvation effects and which in turn would influence the non-radiative decay processes. These extra phenolic groups also enhance its antioxidant properties [36] and this presumably makes it more susceptible to oxidation. Indeed, the fluorescence quantum yield of EGCG is much lower than that of catechin or epicatechin (Table 1) suggesting that the non-radiative rate (k_{IVR}; Fig. 2) dominates in the relaxation of the electronic excited state.

At pH 8, epicatechin also had a two-component fluorescence decay lifetime (see footnote in Supplementary Table). The exact physical origin of the bi-exponential lifetime is unknown. However, it is not uncommon for fluorophores in complex cellular environments to demonstrate multiple decay times as seen in Table 2. Different decay times represent differing physical influences that the nascent electronic excited states are subjected to and consequently may lead to differences in the efficiency of the energy loss process and return to the ground state. The fact that we see a bi-exponential decay indicates that the flavanols find themselves in two differing states and/or two different environments; for example free

294 and bound forms (Supplementary Table). Further investigations studying the ultrafast
295 dynamics will be needed to help explain these differences and/or whether diastereoisomers
296 such as catechin and epicatechin have different fluorescence properties.
297
298 *3.2. Fluorescence lifetime imaging microscopy*
299 *3.2.1. Control experiments with onion cells*
300 The experimental conditions developed above for flavanol solutions were applied initially
301 to onion root cells (tissue soaked in water for 5 h; and followed by two-photon excitation at
302 585 nm). Lifetime decay curves, at several different points in the cells, could be fitted to a
303 single exponential decay giving a τ value between 2.3 and 2.6 ns ($\chi^2 = 1.05$). It is highly
304 likely, however, that under these excitation conditions the emission and lifetime values are
305 mainly due to auto-fluorescence contributions from tryptophan [23]. In order to avoid
306 significant background fluorescence signals from other cellular materials, in particular
307 aromatic amino acids, e.g. tryptophan, when using UV excitation at 290 nm (equivalent to
308 580 nm 2PE excitation) the 2PE excitation wavelength was shifted to 630 nm, which has
309 been shown to give little background interference [23]. Control experiments were then
310 carried out without added flavanols, i.e. in the presence of just water, in order to
311 substantiate that the fluorescence was due to flavanols. The onion sample without added
312 flavanol showed only weak auto-fluorescence and a τ value of 0.8 ns ($\chi^2 = 1.60$) (Fig. 5c)
313 confirming that our FLIM measurements were tracking the flavanol presence in cells (see
314 Section 3.2.2. below). Whole onions are known for their high quercetin concentration (Fig.
315 1) [6], but given the low photon count, we can conclude that neither tryptophan nor

quercetin interfered with flavanol detection, λ_{em}, at 340± 20 nm if 2PE with λ_{ex} was 630 nm.

3.2.2. Absorption of flavanols by onion nuclei

Fig. 5a and 5b show fluorescence lifetime maps of cells in an onion epidermis, which had been soaked in 1 mM aqueous flavanol solutions. Following absorption of catechin or EGCG, the fluorescing nuclei and several bright, small spots of ~ 2 to 7 μm were clearly visible to a much greater extent than the surrounding cell matrix. Careful analysis of Fig. 5b showed a bright spot of 4 μm diameter. It is known that inactive nuclei possess very small nucleoli of the order of ~1 μm [37]. The observed spot is too large to be a nucleolus, we therefore propose that the bright spot was a clustering of perinucleolar organiser regions (NORs) [38]. NORs tend to surround the nucleoli and strongly absorb flavanols [13].

This study demonstrated that FLIM combined with 2PE at 630 nm enabled *in vivo* detection of both catechin and EGCG and avoided interference by tryptophan or quercetin, as the control showed hardly any fluorescence (Fig. 5c). We have previously shown that there is negligible excitation of cellular auto-fluorescence, particular from tryptophan, following multiphoton excitation at 630 nm [23]. Although tryptophan may be excited by multi-photon treatment at 590 nm, which is equivalent to single photon excitation (1PE) at 295 nm, this diminishes by a factor of 10 at 630 nm. Furthermore, the excited state lifetime of tryptophan (~3 ns) is significantly different to that of the flavanols investigated here. These findings, therefore, provided clear and unequivocal evidence for nuclear flavanol absorption. Since the excited state lifetime may be influenced by the environment of the

339 flavanols, the colour trend seen in the FLIM images (Fig. 5a,b) may be due to slight
340 differences in the environment of the absorbed flavanols. A series of *z* axis images taken
341 through a cell revealed that EGCG was detectable throughout the nucleus and not just at the
342 surface (Video Clip S1). EGCG appeared to be concentrated in the NORs; relative
343 proportion of EGCG photon counts were 1 to 3 (cytoplasm) : 10 (nucleus) : 100 to 150
344 (NORs) (*data not shown*).
345
346 *3.3. FLIM lifetimes of bound versus free flavanols in solution*
347 Fluorescence decay curves of nucleus-bound catechin were best fitted to two components,
348 i.e. τ_1 = 0.5 ns (77.5%) and τ_2 = 2.7 ns (22.5%; χ^2 of 1.04) (Table 2). It is unlikely that τ_2
349 emanates from tryptophan as the same experiments with EGCG fitted to a single
350 component decay with an average τ of 0.25 ± 0.05 ns (Table 2). The increase in EGCG
351 lifetime from <0.045 ns in solution (Fig. 4) to 0.25 ns in the nucleus is a reverse of the
352 trend seen for catechin, which showed a lifetime of ~ 1 ns in solution and 0.5 ns in the
353 nucleus.
354
355 The effect of nuclear association generating different lifetimes is given in Table 2 and was
356 recorded when Fig. 5 was taken. Taken together, these observations suggest that the two
357 flavanols (catechin and EGCG) may differ in their interaction mechanisms with nuclear
358 components. The lowering of a lifetime indicates either an enhanced non-radiative decay
359 (through for example formation of hydrogen bonds) [31] or possibly self-association which
360 has been reported for catechin [39]. A decrease in lifetimes upon cellular absorption has
361 also been reported for 5-hydroxytryptophan and was attributed to self-quenching or

environmental effects [23]. Further research will be needed to establish whether oxidation during the cellular absorption experiment could have contributed to the shorter catechin lifetime (Fig. 3) and whether oxidation would have increased EGCG fluorescence lifetime. It seems, however, more likely that this contrasting lifetime behaviour is indicative of different interaction mechanisms.

3.4. Endogenous flavanols in Taxus baccata

The same 2PE experimental conditions were then applied to pollen mother cells which had been isolated from microspores of male *Taxus baccata* cones. According to Feucht *et al.* [14] late tetrads and early microspores possess endogenous catechin and epicatechin. We observed, however, fluorescence lifetimes, which could be fitted to single component decays with τ of 0.2 ns and which resembled EGCG, rather than catechin or epicatechin (Table 2). Interestingly, the photon count of the signal to noise ratio from endogenous flavanols in the *Taxus* cells was not dis-similar to onion cells soaked in a 1 mM EGCG solution. Younger cones at the tip of the *Taxus baccata* twig yielded twice as many photons compared to slightly more mature cones from further along the twig. This finding agrees with previous observations [14,15] that nuclear DMACA staining for flavanols was most intense during high cell activity, e.g. in mitotic and stem cells. Interestingly, it also coincides with observations of higher EGCG concentrations in foetal than maternal plasma of rats: absorbed catechins were found in the brain, eye, heart, lung, kidney, liver and placenta of fetal organs [40].

3.5. Flavanol fluorescence lifetimes in the presence of DNA or histone proteins

385 The fact that flavanols bind to the nucleus raises an important question: which nuclear
386 components act as the binding sites? Several previous studies demonstrated that DNA
387 interacts with planar flavonoids, such as flavonols and anthocyanidins, and depending on
388 the experimental conditions, these interactions were either weak or led to intercalation [41].
389 However, flavanols are *not* planar and may therefore not be able to intercalate with DNA.
390 We, therefore, explored fluorescence lifetime behaviour of flavanols in the presence of
391 DNA. Addition of DNA had no effect on catechin or epicatechin lifetimes in aqueous
392 solutions (2 mM; pH 8 in Tris buffer; data not shown). This agrees with results from UV-
393 Vis spectroscopic titrations which also found that DNA did not interact with catechin or
394 EGCG in 0.1 M Tris at pH 7.4 or 8.0 [16].
395
396 However, Polster *et al.* [16] reported that histone proteins might be the nuclear targets for
397 catechin and EGCG. Using UV-Vis titration experiments, they showed that both flavanols
398 bound to histone sulphate and interactions were more pronounced at pH 8.0 than 7.4 in Tris
399 buffer. Since these titration experiments required approximately 1 h in total [42], it could be
400 argued that this might be sufficient time for oxidative reactions and artefact formation to
401 occur especially at higher pH values as determined in Fig. 3. The present fluorescence
402 lifetime measurements were, however, made within 30 s of mixing the flavanol and histone
403 solutions (note: the fluorescence lifetime experiments were also done in Tris buffer, as the
404 UV-Vis titrations revealed that histone sulphate showed a less pronounced interaction with
405 catechin in phosphate than Tris buffer [16]).
406

The lifetimes of catechin and epicatechin in the presence of histone proteins were investigated at two concentrations (1.1 and 1.9 mM) and pH (7 and 8) (Supplementary Table). Given the short lifetimes recorded and the errors in fitting bi-exponential decays, the data for the different flavanols need careful interpretation. At this stage we are unable to clearly identify whether or not histones bind to flavanols, which would be expected to be shown by a change in lifetime (i.e. due to quenching). From other work it is, however, also clear that histone preparations differ in their ability to associate with flavanols [13] and, therefore, further fluorescence studies will be needed. Nevertheless, these initial findings demonstrate the potential power of studying flavanol–histone interactions by fluorescence methods. It is now also evident that much fundamental work is needed for characterising how the chemical environment (including pH and oxygen concentration) influence fluorescence lifetimes, quantum yields and spectra of flavanols. With regard to pH, the pK_a values of catechin, for example, are *ca.* 8.6 and 9.4 [43] and thus at pH 8 three different protolyte species exist for catechin: BH_2, BH^-, and B^{2-}. The fluorescence behaviour of each of these species will need to be understood and only through such careful measurements can these types of fluorescence measurements provide the much needed tool for elucidating the interactions between flavanols, histones and DNA.

3.6. Possible role of nuclear flavanols beyond an antioxidant function

Nuclear absorption has been reported not only for flavanols [13] but also for some other flavonoids. *Arabidopsis thaliana* nuclei absorb flavonols [44.45], *Drosophila* follicle nuclei absorb quercetin [46] and *Flaveria chloraefolia* nuclei absorb sulfonated flavanols [47]. It used to be widely accepted that the major function of polyphenols such as flavonoids was

to protect DNA against UV damage and oxidative stress, but this has now been questioned [8,10]. Instead they were shown recently also to affect cell signalling and gene expression [48,49]. Flavanols are involved in the transcriptional activation of genes and modulation of epigenetic changes [36,50].

Whilst several dietary flavonols and the green tea flavanol, EGCG, have been implicated in interacting and protecting DNA against damage [41,51, 52], the fact that they inhibit DNA methyltransferases *in vitro* and *in vivo* at the μmolar to sub-μmolar level is potentially more important for their effects on health [5,7,29,48,53]. Moreover, EGCG was also a potent inhibitor of histone acetyltransferase [50]. Histone acetylation has previously been shown to affect flavanol association [13,16] and is known to alter the chromatin structure, which in turn has been linked to the transcriptional activation of genes [15]. Both processes, DNA methylation and histone acetylation, are involved in epigenetic changes [54]. Indeed, Yamada *et al.* [53] concluded that EGCG may have inhibitory effects on the epigenetic changes that occur during carcinogenesis and aging. Whilst we found no evidence for interactions between flavanols and DNA, the results presented here in terms of flavanol association and penetration through the nucleus do not rule out the possibility that histones may be a target for EGCG, catechin and epicatechin. Solution phase ultrafast structure and dynamics studies such as time resolved infra-red (IR) or time resolved 2-dimensional IR will be needed to probe the origin of the bi-exponential lifetimes, which differed between the three flavanols. Such time resolved spectroscopic techniques will indicate the functional groups responsible for the fast dynamics that differ amongst these flavanols.

3.7. Future prospects

Given the recent discoveries identifying that flavanols may well be involved in epigenetic changes, highly sensitive techniques will be needed to trace their uptake and trafficking at the sub-cellular and sub-nuclear level and at physiologically relevant concentrations. Our results suggest that not all flavanols will interact via the same molecular mechanism and this will require new techniques with sufficient specificity and sensitivity. New developments in fluorescence lifetime imaging techniques and ultra-fast spectroscopy, as demonstrated here, may hold the key and pave the way for studying their functions and synthesis in plant cells. The trafficking, uptake and subcellular localisation of flavanols is of acute interest also for current research on tannin synthesis in plants [55]. Unravelling this last hurdle of flavonoid biosynthesis, storage and release would facilitate the development of new plant varieties with tannin compositions that can offer enhanced biological activities for nutrition and health [11].

Such analytical developments will facilitate new types of biological experiments that can test how these compounds, when present in plant foods, can impact on mammalian cells and health. Although FLIM is a new technique to both mammalian and plant cell biologists alike, its application is growing rapidly [23-26,28], particularly in protein-protein interactions that involve energy transfer processes. However, this is the first study to report FLIM for other plant components and as the technique becomes more readily available, its impact can only grow. This study has shown that relatively small changes in flavanol structures (EGCG *versus* catechin or epicatechin; Fig. 1) lead to measurable changes in lifetime behaviour in the free and bound states. As plants synthesise several types of flavonoids, that vary in oxidation and substitution patterns [1], it is expected that other

flavonoid compounds will be detectable using different combinations of excitation and emission wavelengths.

4. Conclusions

In conclusion, 2-photon excitation at 585 and 630 nm has enabled for the first time the measurement of fluorescence lifetimes from three flavanols, catechin, epicatechin and EGCG, in solution and *in vivo*. Lifetimes ranging from <45 ps to 1 ns in solution have been determined. *In vivo* experiments with onion cells demonstrated that tryptophan and quercetin have sufficiently low absorbance at 630 nm and this allowed the detection of externally added and endogenous flavanols within *Allium cepa* and *Taxus baccata* cells. Interestingly, fluorescence decay curves of catechin and EGCG differed markedly both in solution and when bound at the nucleus. This fact could be used in the future for selectively tracing the different flavanols *in vivo*. Furthermore, this work demonstrates how the application of fluorescence lifetime technology may be used to investigate the way flavanols interact with individual cellular components. We also conclude that flavanols are absorbed by cell nuclei and this provides new research challenges with regard to their intracellular functions.

Semi-quantitative measurements revealed that the relative ratios of EGCG concentrations in perinucleolar organiser regions : nucleus : cytoplasm were approximately 100:10:1. Moreover, 3-D FLIM showed that externally added EGCG penetrated the whole nucleus of onion cells and was not just absorbed on the surface. The FLIM technique described here proved therefore a significant advance to DMACA staining and is capable of providing

quantitative biophysical information to probe the intra-cellular functions of flavanols such as EGCG, which is the major flavanol of green tea.

Acknowledgements

We are grateful to the Science and Technology Facilities Council for facility access time and financial support (No 81072) and to Professor R.H. Bisby, Salford University, for helpful discussions.

References

[1] J.A.M. Kyle, G.G. Duthie, in: Ø.M. Anderson, K.R. Markham (Eds.), Flavonoids: Chemistry, Biochemistry and Applications, CRC Press, Boca Raton, 2006, pp. 219-255.

[2] P.J. Hernes, J.I. Hedges, Geochim. Cosmochim. Acta. 68 (2004) 1293–1307.

[3] R.M. Hackman, J.A. Polagruto, Q.Y. Zhu, B. Sun, H. Fujii, C.L. Keen, Phytochem. Rev. 7 (2008) 195-208.

[4] J.D. Lambert, R.J. Elias, Arch. Biochem. Biophys. 501 (2010) 65-72.

[5] S. Sang, J.D. Lambert, C.S. Yang, J. Sci. Food Agric. 86 (2006) 2256-2265.

[6] G. Williamson, C. Manach, Am. J. Clin. Nutr. 81 (suppl) (2005) 243S–55S.

[7] W.J.L. Lee, J.-Y. Sim, B.T. Zhu, Mol. Pharmacol. 68 (2005) 1018-1030.

[8] M. Clifford, J.E. Brown, in: Ø.M. Anderson, K.R. Markham (Eds), Flavonoids: Chemistry, Biochemistry and Applications, CRC Press, Boca Raton, 2006, pp. 319-370.

[9] B. Holst, G. Williamson, Curr. Opin. Biotechnol. 18 (2008) 73-82.

[10] I. Hernández, L. Alegre, F. Van Breusegem, S. Munné-Bosch, Trends Plant Sci. 14 (2009) 125-132.

[11] I. Mueller-Harvey, J. Sci. Food Agric. 86 (2006) 2010-2037.

[12] J.D. Lambert, J. Hong, G.-Y. Yang, J. Liao, C.S. Yang, Am. J. Clin. Nutr. 81 (suppl.) (2005) 284S-291S.

[13] W. Feucht, H. Dithmar, J. Polster, Internat. J. Mol. Sci. 8 (2007) 635-650.

[14] W. Feucht, D. Treutter, H. Dithmar, J. Polster, Tree Physiol. 28 (2008) 1783-1791.

[15] W. Feucht, H. Dithmar, J. Polster, J. Bot. (2009) Article ID 842869 (doi: 10.1155/2009/842869)

[16] J. Polster, H. Dithmar, W. Feucht, Biol. Chem. 384 (2003) 997-1006.

[17] J. Bauer, K. Neubauer, H. Dithmar, J. Polster, W. Feucht, Adv. Food Sci. 31 (2009) 82-88.

[18] J. Polster, H. Dithmar, R. Burgemeister, G. Friedemann, W. Feucht, Physiol. Plant. 128 (2006) 163-174.

[19] D. Treutter, J. Chromatogr. 467 (1989) 185-193.

[20] A.-P. Nifli, P.A. Theodoropoulos, S. Munier, C. Castagnino, E. Roussakis, H.E. Katerinopoulos, J. Vercauteren, E. Castanas, J. Agric. Food Chem. 55 (2007) 2873-2878.

[21] K. Suhling, P.M. French, D. Phillips, Photochem. Photobiol. Sci. 4 (2005) 13-22.

[22] E.B. van Munster, T.W.J. Gadella, Adv. Biochem. Eng. Biotechnol. 95 (2005) 143-175.

[23] S.W. Botchway, A.W. Parker, R.H. Bisby, A.G. Crisostomo, Microsc. Res. Tech. 71 (2008) 267-273.

[24] A. Osterrieder, C.M. Carvalho, M. Latijnhouwers, J.N. Johansen, C. Stubbs, S. Botchway, C. Hawes, Traffic. 10 (2009) 1-13.

[25] R.H. Bisby, S.W. Botchway, A.G. Crisostomo, J. Karolin, A.W. Parker, L. Schröder, Spectroscopy 24 (2010) 137-142.

[26] S.W. Botchway, M. Charnley, J.W. Haycock, A.W. Parker, D.L. Rochester, J.A. Weinstein, J.A.G. Williams, PNAS, 105 (2008) 16071-16076.

[27] P.T.C. So, C.Y. Dong, B.R. Masters, K.M. Berland, Annu. Rev. Biomed. Eng. 2 (2000) 399-429.

[28] I. Sparkes, N. Tolley, I. Aller, J. Svozil, A. Osterrieder, S. Botchway, C. Mueller, L. Frigerio, C. Hawes, Plant Cell 22 (2010) 1333-1343.

[29] A. Rajavelu, Z. Tulyasheva, R. Jaiswal, A. Jeltsch, N. Kuhnert, BMC Biochemistry 12:16 (2011) Doi:10.1186/1471-2091-12-16.

[30] W. Feucht, J. Polster, Z. Naturforsch. 56c (2001) 479-481.

[31] J.R. Lakowicz, Principles of Fluorescence Spectroscopy, fourth ed., Springer, New York, 2006.

[32] D.F. Eaton, Pure Appl. Chem. 60 (1988) 1107-1114.

[33] Website: http://omlc.ogi.edu/spectra/PhotochemCAD/html/tryptophan.html

[34] S. Sang, M.-J. Lee, Z. Hou, C.-T. Ho, C.S. Yang, J. Agric. Food Chem. 53 (2005) 9478-9484.

[35] N.P. Slabbert, Tetrahedron 33 (1977) 821-824.

[36] M.A. Soobrattee, V.S. Neergheen, A. Luximon-Ramma, O.I. Aruoma, T. Bahorun, Mutation Res. 579 (2005) 200-213.

[37] A.V. Probst, P.F. Fransz, J. Pazkowski, O. Mittelsten-Scheid, Plant J. 33 (2003) 743-749.

[38] D. Hernandez-Verdun, J. Cell Sci. 99 (1991) 465-471.

[39] F.L. Tobiason, R.W. Hemingway, G. Vergoten, Basic Life Sci. 66 (1999) 527-544.

[40] K.O., Chu, C.C. Wang, C.Y. Chu, K.W. Choy, C.P. Pang, M.S. Rogers, Hum. Reprod. 22 (2007) 280-287.

[41] C.D. Kanakis, P.A. Tarantilis, M.G. Polissiou, S. Diamantoglou, H.A. Tajmir-Riahi, Cell Biochem. Biophys. 49 (2007) 29-36.

[42] W. Feucht, H. Dithmar, J. Polster, Plant Biol. 6 (2004) 696-701.

[43] M.B. Inoue, M. Inoue, Q. Fernando, S. Valcic, B.N. Timmermann, J. Inorg. Biochem. 88 (2002) 7-13.

[44] W.A. Peer, D.E. Brown, B.W. Tague, G.K. Muday, L. Taiz, A.S. Murphy, Plant Physiol. 126 (2001) 536-548.

[45] D.E. Saslowsky, U. Warek, B.S.J. Winkel, J. Biol. Chem. 280 (2005) 23735-23740.

[46] H.O. Gutzeit, Y. Henker, B. Kind, A. Franz, Biochem. Biophys. Res. Commun. 318 (2004) 490-495.

[47] J. Grandmaison, R. Ibrahim, J. Plant Physiol. 147 (1996) 653-660.

[48] M.Z. Fang, Y. Wang, N. Ai, Z. Hou, Y. Sun, H. Lu, W. Welsh, C.S. Yang, Cancer Res. 63 (2003) 7563-7570.

[49] T.M. Ehrman, D.J. Barlow, P.J. Hyland, J. Chem. Inf. Model 47 (2007) 254-263.

[50] K.-C. Choi, M.G. Jung, Y.-H. Lee, J.C. Yoon, S.H. Kwon, H.-B. Kang, M.-J. Kim, J.-H. Cha, Y.J. Kim, W.J. Jun, J.M. Lee, H.-G. Yoon, Cancer Res. 69 (2009) 583-592.

590 [51] M. Glei, B.L. Pool-Zobel, Toxicol. in Vitro 20 (2005) 295-300.
591 [52] L. Guo, L.H. Wang, B. Sun, J.Y. Yang, Y.Q. Zhao, Y.X. Dong, M.I. Spranger, C.F.
592 Wu, J. Agric. Food Chem. 55 (2007) 5881-5891.
593 [53] H. Yamada, H. Sugimura, T. Tsuneyoshi, J. Food Agric. Environ. 3 (2005) 73-76.
594 [54] J. Ordovás, C.E. Smith, Nature Rev. Cardiol. 7 (2010) 510-519.
595 [55] J. Zhao, Y. Pang, R.A. Dixon, Plant Physiol. 153 (2010) 437-443.
596

Legend to Figures

Fig. 1:

Structures of three flavanols, catechin (**1**), epicatechin (**2**), and epigallocatechin gallate (**3**), and one flavonol, quercetin (**4**) (*note*: A, B, C denote the flavonoid rings).

Fig. 2:

The Jablonski diagramme depicting the energy levels of a molecule. S_o represents the ground singlet states, S_1, S_2 the excited singlet states; T_1 the triplet excited states. Electronic levels are subdivided into vibrational levels ($v_1, v_2 \ldots v_n$). IC indicates internal conversion, $k_{fluorescence}$: rate of fluorescence leading from S_1 ($v_1 = 0$) to S_o (v_1 or v_n), k_{IVR}: intramolecular vibrational relaxation, k_{ISC}: rate of intersystem crossing and k_{quench}: rate of reaction with other molecules, chemical or energy transfer.

Fig. 3:

Time course of fluorescence lifetimes (ns) of catechin (2 mM) in 0.1 M phosphate buffer in air or nitrogen atmospheres at pH 5.8, 7.1 and 8.2 (λ_{ex} = 585 nm).

Fig. 4:

Fluorescence decay curves of catechin, epicatechin and epigallocatechin gallate (EGCG) solutions (2 mM) in 0.1 M phosphate buffer at pH 8.1 (λ_{ex} = 585 nm).

Fig. 5:

Fluorescence lifetime images (λ_{ex} = 630 nm) of a cell from an onion epidermis soaked in 1 mM aqueous solutions of a) catechin (τ_1 = 0.4 ns (82%), τ_2 = 2.6 ns (18%)), b) epigallocatechin gallate (τ = 0.2 ns) and c) control in water without added flavanol. Image (A) shows a steady state image of the total emission lifetimes and image (B) shows the analysed fluorescence excited state map. The distribution of fluorescence lifetimes in (B) is illustrated in image (C), where the vertical axis represents the frequency and the horizontal axis represents lifetime in pico-seconds. (*Note*: control nucleus shows hardly any fluorescence in Fig. 5c).

Supporting information

Additional Supporting Information may be found in the online version of this article:

Supplementary Table: Fluorescence lifetimes (ns) of flavanols in the presence of different histones (Tris buffers, pH 7 and 8). Pre-exponential factors are shown in brackets.

Fig. S1. UV-Vis spectra of catechin, epicatechin and epigallocatechin gallate recorded from 200 to 595 nm.

Video Clip S1. 3D stack of multiphoton excited (λ_{ex} = 630 nm) fluorescence image from an onion cell epidermis soaked in a 1mM aqueous solution of epigallocatechin gallate. Images were recorded at 0.5 - 2.0 μm slices.

Please note: Wiley Blackwell are not responsible for the content or functionality of any supporting materials supplied by the authors. Any queries (other than missing material) should be directed to the corresponding author for the article.

Table 1

Fluorescence quantum yields of catechin, epicatechin and epigallocatechin gallate (EGCG) in methanol at 37 ºC.

Compound	**Quantum yield[a]**
Catechin	0.018
Epicatechin	0.015
EGCG	0.003

[a] Estimated accuracy = ±16%

Table 2

Fluorescence lifetimes (ns) and pre-exponential factors (A_1 and A_2) of externally added flavanols, which were absorbed by onion epidermis, and endogenous flavanols in *Taxus baccata* male cones (± standard deviations).

Sample	τ_1 (ns)	A_1 %	τ_2 (ns)	A_2 %
Onion epidermis:				
control in water	0.84 [a]	100		
Onion epidermis:				
+ catechin	0.5 ± 0.04	77.5 ± 6.92	2.7 ± 0.19	22.5 ± 6.92
+ epigallocatechin gallate (EGCG)	0.25 ± 0.05	99.2 ± 1.13		
Taxus baccata male cones:				
in water	0.2 ± 0.03	93.4 ± 6.46	0.5 ± 0.2	6.6 ± 6.46

[a] The control had a very low photon count in the absence of externally added flavanols and the data were quite noisy (see Fig. 5c), therefore it was not possible to obtain a standard deviation of the background lifetime.

Figure 1:

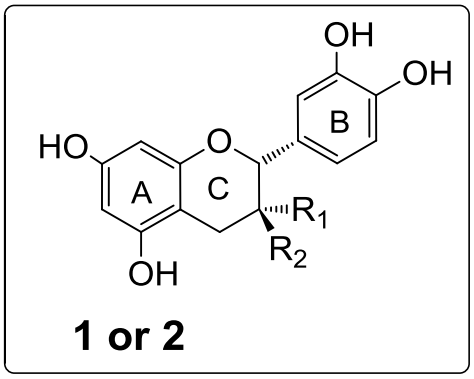

1 or 2

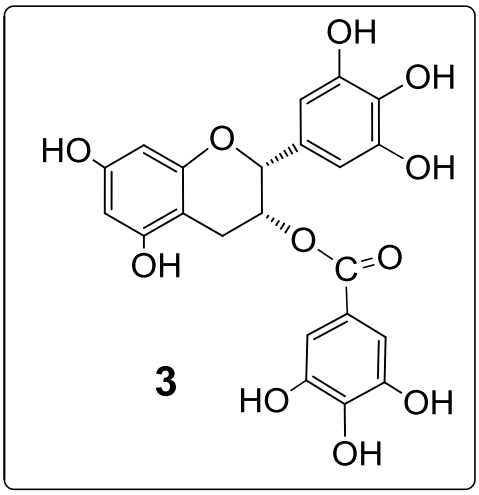

3

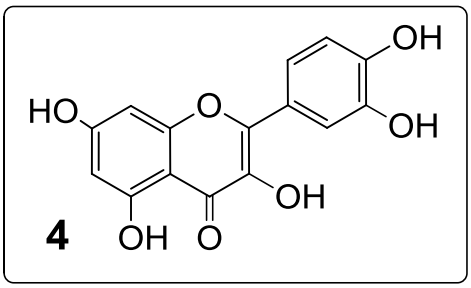

4

669 Fig 2
670

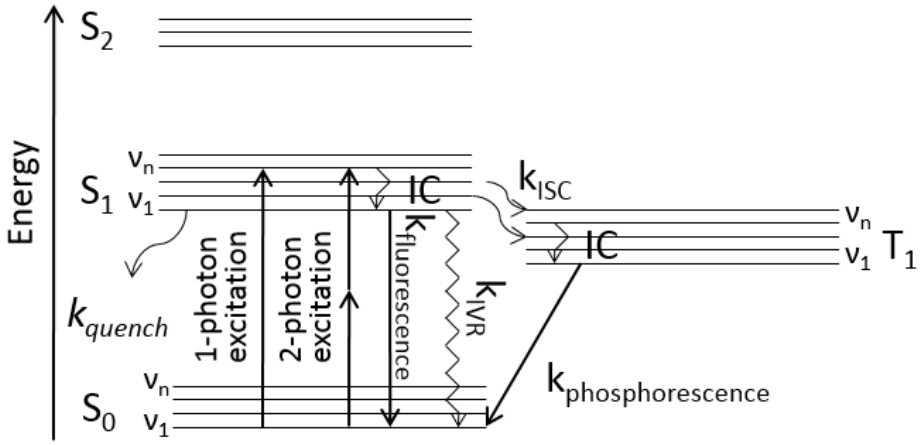

671
672
673 Fig 3
674

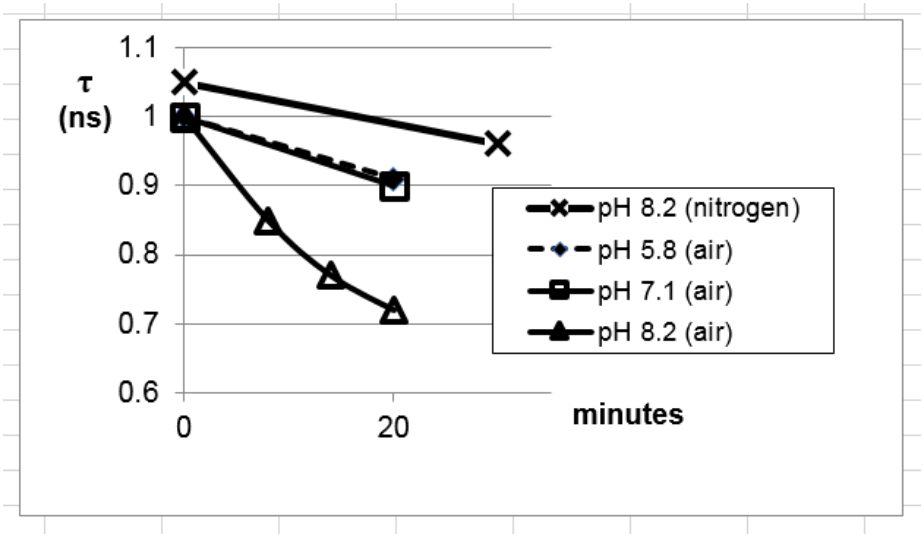

675
676

677 Fig 4

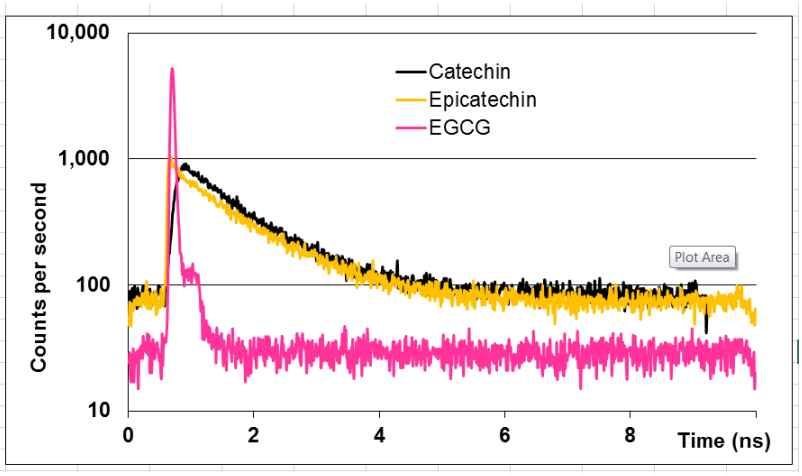

678

679

Fig 5a

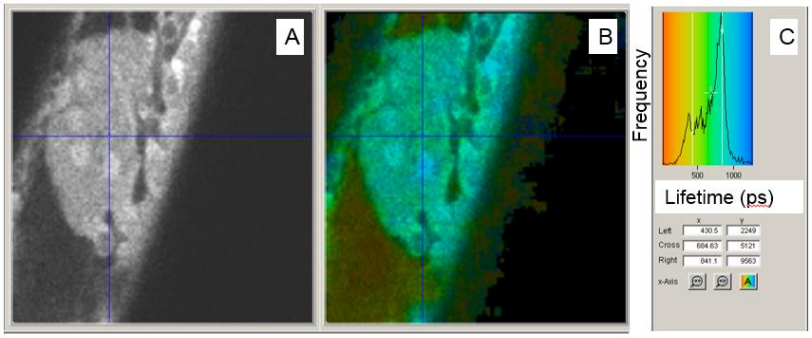

Fig 5 b

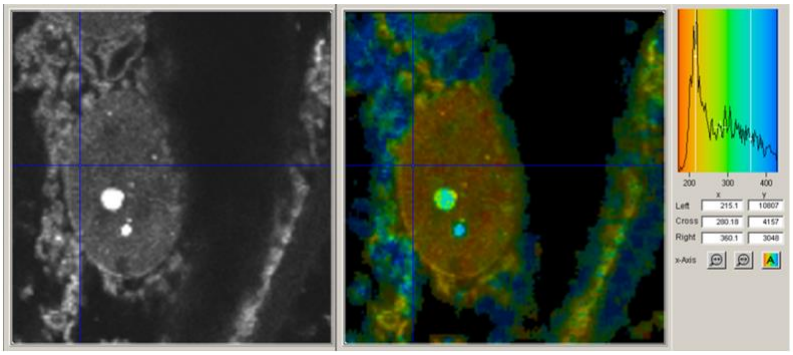

Fig 5c

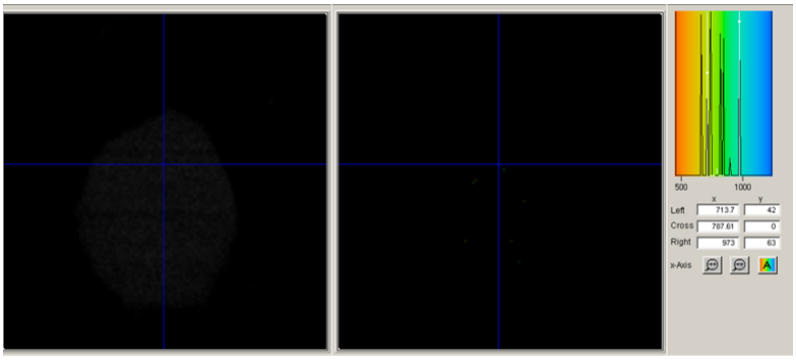

Fig S1

Figure S1: UV-Vis spectra of catechin, epicatechin and epigallocatechin gallate recorded from 200 to 595 nm.

Catechin

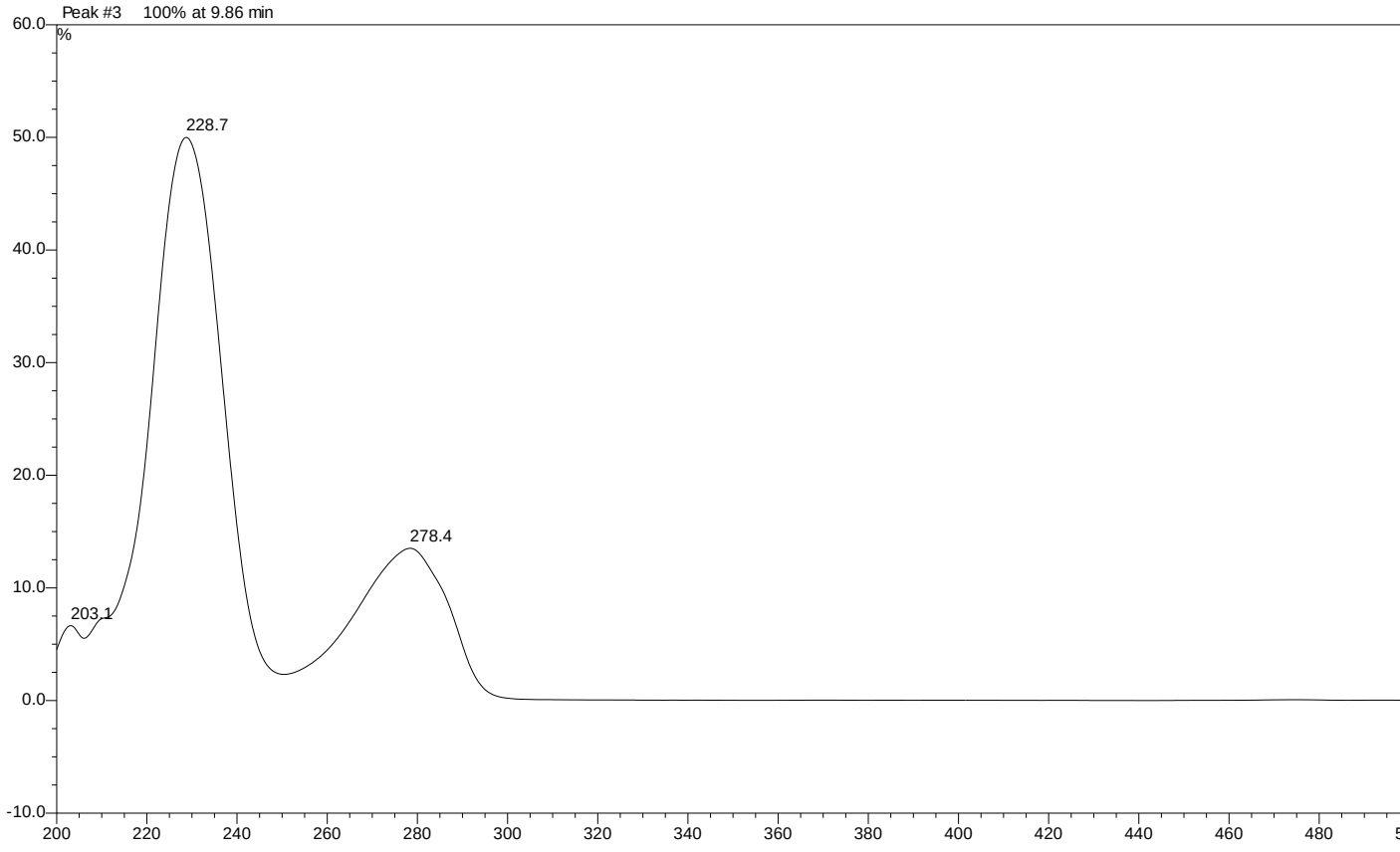

Epicatechin

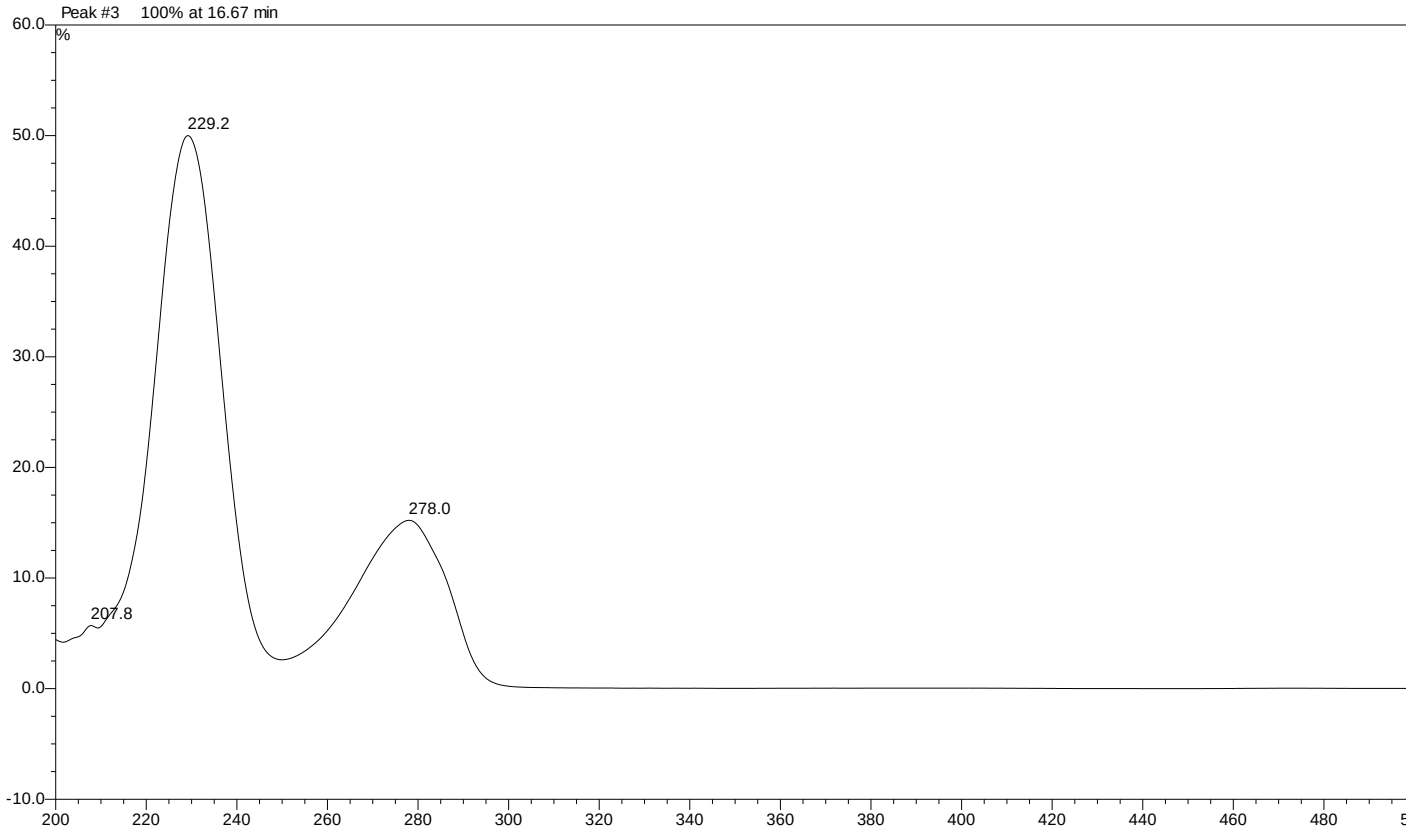

Epicatechin gallate

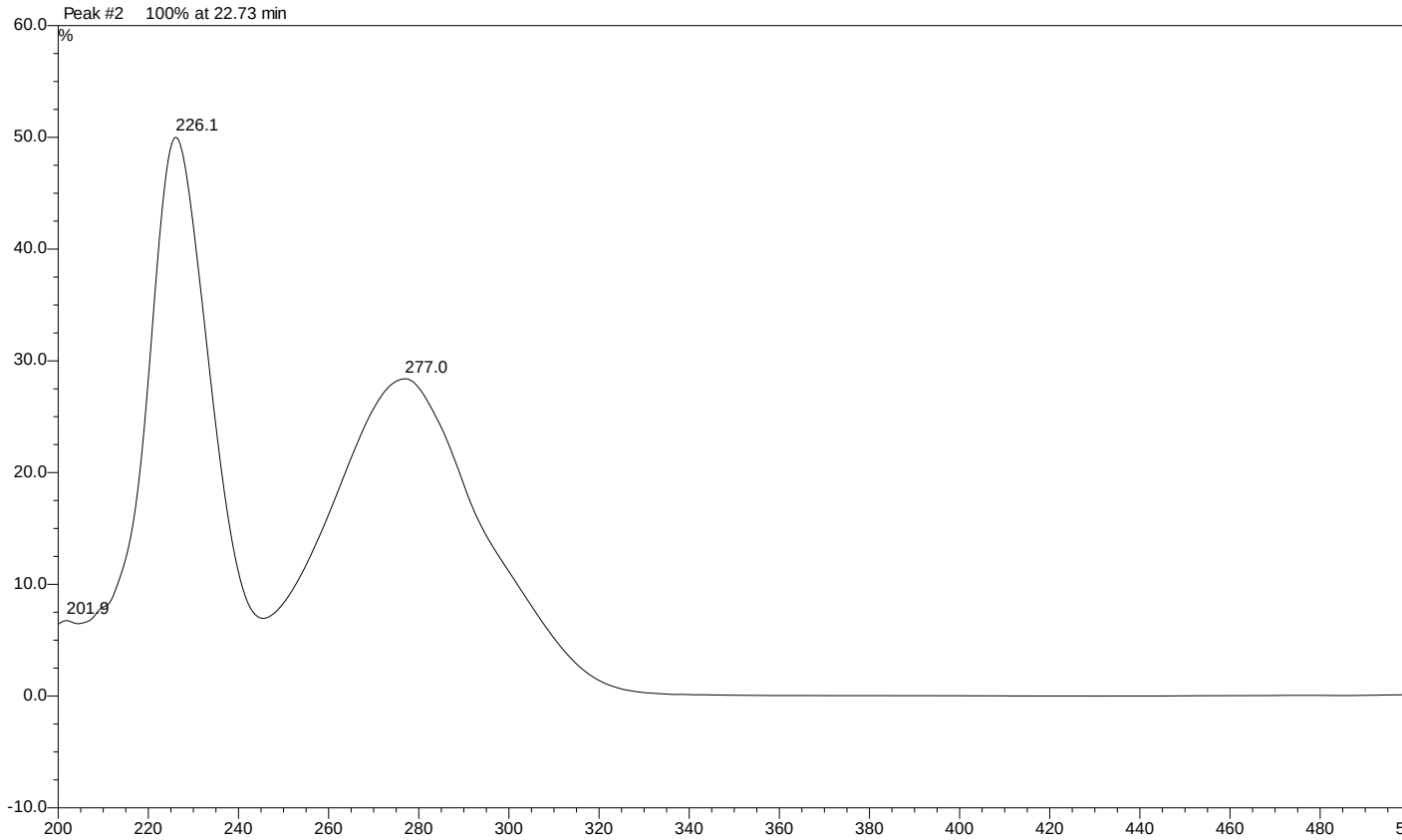

Supplementary **Table**

Fluorescence lifetimes (ns) of flavanols in the presence of different histones (Tris buffers, pH 7 and 8). Pre-exponential factors are shown in brackets.

	1 mM Flavanol				**2 mM Flavanol**			
	pH 7		**pH 8**		**pH 7**		**pH 8** [b]	
	τ_1 [a]	**τ_2**	**τ_1**	**τ_2**	**τ_1**	**τ_2**	**τ_1**	**τ_2**
(+)-Catechin [b]								
+ Sigma histone	0.9 (75%)	1.9 (25%)	0.9 (92%)	2.5 (8%)	1.1 (82%)	1.7 (18%)	1.1 (80%)	1.9 (20%)
+ Histone sulphate	1.1 (95%)	4.0 (5%)	0.9 (75%)	2.0 (25%)	1.1 (88%)	2.1 (12%)	1.1 (88%)	2.0 (12%)
+ Roche histone	1.0 (96%)	3.5 (4%)	0.9 (80%)	2.7 (20%)	0.8 (86%)	2.5 (14%)	1.1 (93%)	3.2 (7%)
(-)-Epicatechin [b]								
+ Sigma histone	0.8 (75%)	2.0 (25%)	0.9 (90%)	2.5 (10%)	1.1 (85%)	1.8 (15%)	1.0 (86%)	2.0 (14%)
+ Histone sulphate	nd[c]	nd	nd	nd	1.1 (87%)	1.9 (13%)	1.0 (84%)	1.9 (16%)
+ Roche histone	1.0 (92%)	2.8 (10%)	0.9 (80%)	2.3 (20%)	1.1 (90%)	3.1 (10%)	1.0 (90%)	2.7 (10%)
Average	0.9	2.4	0.9	2.3	1.1	2.3	1.1	2.4

[a] Experimental error is ±50 ps; [b] For comparison, lifetime measurements in 0.1 M phosphate buffer at pH 8.1 gave τ = 1.0 ns for catechin and τ_1 = 1.1 (72%) and τ_2 = 0.1 ns (28%) for epicatechin (note: Due to the poor signal-to-noise at longer times the errors are significantly larger for the second lifetime (τ_2) and the pre-exponential factors of less than 10% may be due to a fluorescence contribution from impurities); [c] nd = not determined.